HHS Public Access

Author manuscript

Dev Neurosci. Author manuscript; available in PMC 2018 April 04.

Published in final edited form as:

Dev Neurosci. 2017 ; 39(6): 487–497. doi:10.1159/000480428.

Impaired Cerebellar Maturation, Growth Restriction, and Circulating Insulin-Like Growth Factor 1 in Preterm Rabbit Pups

Kristbjörg Sveinsdóttir[a], **John-Kalle Länsberg**[a], **Snjólaug Sveinsdóttir**[a], **Martin Garwicz**[c], **Lennart Ohlsson**[d], **Ann Hellström**[e], **Lois Smith**[f], **Magnus Gram**[b], and **David Ley**[a]

[a]Department of Pediatrics, Lund University, Gothenburg, Sweden

[b]Department of Infection Medicine, Lund University, Gothenburg, Sweden

[c]Neuronano Research Center, Lund University, Gothenburg, Sweden

[d]Department of Micromorph AB, Lund, Gothenburg, Sweden

[e]Department of Ophthalmology, Institute of Neuroscience and Physiology, Sahlgrenska Academy, University of Gothenburg, Gothenburg, Sweden

[f]Department of Ophthalmology, Boston Children's Hospital, Boston, MA, USA

Abstract

Cerebellar growth is impeded following very preterm birth in human infants and the observed reduction in cerebellar volume is associated with neurodevelopmental impairment. Decreased levels of circulating insulin-like growth factor 1 (IGF-1) are associated with decreased cerebellar volume. The relationship between preterm birth, circulating IGF-1, and key cell populations supporting cerebellar proliferation is unknown. The aim of this study was to evaluate the effect of preterm birth on postnatal growth, circulating IGF-1, and cerebellar maturation in a preterm rabbit pup model. Preterm rabbit pups (PT) were delivered by cesarean section at day 29 of gestation, cared for in closed incubators with humidified air, and gavage fed with formula. Control term pups (T) delivered by spontaneous vaginal delivery at day 32 of gestation were housed and fed by their lactating doe. In vivo perfusion-fixation for immunohistochemical evaluation of cerebellar proliferation, cell maturation, and apoptosis was performed at repeated time points in PT and T pups. Results show that the mean weight of the pups and circulating IGF-1 protein levels were lower in the PT group at all time points ($p < 0.05$) than in the T group. Postnatal weight development correlated with circulating IGF-1 ($r^2 = 0.89$) independently of gestational age at birth and postnatal age. The proliferative (Ki-67-positive) portion of the external granular layer (EGL) was decreased in the PT group at postnatal day 2 (P2) compared to in the T group ($p = 0.01$). Purkinje cells exhibited decreased calbindin staining at P0 ($p = 0.003$), P2 ($p = 0.004$), and P5 ($p = 0.04$) in the PT group compared to in the T group. Staining for sonic hedgehog was positive in neuronal EGL progenitors and Purkinje cells at early time points but was restricted to a well-defined Purkinje cell monolayer at later time points. Preterm birth in rabbit pups is associated with lower circulating levels of IGF-1, decreased postnatal growth, and decreased cerebellar EGL proliferation and Purkinje cell maturation. The preterm rabbit pup model exhibits important

David Ley, MD, PhD, Lund University, Skane University Hospital, Department of Clinical Sciences, Pediatrics, BMC C14, SE–221 84 Lund (Sweden), david.ley@med.lu.se.

characteristics of human preterm birth, and may thus be suitable for the evaluation of interventions aiming to modify growth and cerebellar development in the preterm population.

Keywords

Preterm birth; Cerebellum; Insulin-like growth factor 1; Purkinje cells; Sonic hedgehog protein

Introduction

The improved survival of very preterm infants has increased the awareness that very preterm birth is associated with diverse neurodevelopmental disability [1–3]. The knowledge on brain development following preterm birth is insufficient. Acquired lesions such as intraventricular hemorrhage and white-matter damage of the cerebrum have well-defined implications for neurodevelopmental impairment. However, the mechanisms whereby very premature birth per se has a damaging effect on brain development remain less well defined.

The use of magnetic resonance imaging has increased awareness of cerebellar abnormalities following preterm birth and their important contribution to neurodevelopmental disability. In humans, the cerebellum is the fastest-growing part of the brain during late pregnancy. The cerebellar volume increases 5-fold and the surface area increases 30-fold during the 3rd trimester. Consequently, very premature birth may have important implications for the structural and functional integrity of the cerebellum.

In very preterm human infants, the cerebellar volume, as determined by magnetic resonance imaging, is smaller at term age than in control term infants [4, 5]. The observed reduction in cerebellar volume has been associated with acquired brain insults such as intraventricular hemorrhage [6, 7], but is also present in relation to extreme prematurity per se [4, 8]. Importantly, reduced cerebellar volume at term age has been associated with subsequent neurological impairment [6, 9, 10].

The mechanisms involved in reduced cerebellar volume following very preterm birth remain unknown. We have shown that very preterm birth is followed by decreased circulating levels of insulin-like growth factor 1 (IGF-1) [11]. Continued study showed that decreased levels of IGF-1 were associated with decreased brain volumes at term age, with the cerebellum exhibiting the strongest correlation [4]. Proliferation of granule cell precursors in the external granular layer (EGL) and their inward movement to form the internal granular layer (IGL) constitute a critical event in cerebellar development [12]. Sonic hedgehog (Shh), a mitotic factor secreted by Purkinje neurons, is responsible for the growth and patterning of the cerebellum [13]. IGF-1, an anabolic and neuroprotective factor, is essential for fetal growth and pre- and postnatal brain development [14]. IGF-1 has been suggested to have a supporting role in Shh-induced proliferation of EGL precursor cells [15].

We hypothesized that preterm birth and the subsequent loss of placental support with a resulting decrease in circulating levels of IGF-1, may be essential, and partly causal, in the decreased cerebellar growth observed in very preterm infants.

Greater understanding of these relationships would be facilitated by an animal model that incorporates preterm birth. To date, few, if any, reported animal models incorporate the premature loss of placental support during a window of brain maturation corresponding to that of the very preterm human infant. The preterm rabbit pup model could be such an animal model since a significant part of the EGL proliferation takes place prior to birth, as opposed to mice and rats where EGL proliferation is mainly postnatal.

We thus aimed to evaluate if preterm delivery of rabbit pups would result in decreased circulating levels of IGF-1, and if preterm delivery per se would result in maturational changes in key elements of the developing cerebellum.

Material and Methods

The Preterm Rabbit Pup Model

The animal protocol was approved by the Swedish Animal Ethics Committee in Lund. The study included 64 rabbit pups from 16 litters. A half-breed between the New Zealand White and Lop was used. The preterm (PT) rabbit pups were delivered by cesarean section at gestational day 29 (term 32 days) after the does were anesthetized with i.v. propofol (5 mg/kg) and local infiltration of the abdominal wall using Lidocaine with adrenaline (10 mg/mL + 5 μl/mL). After birth, the pups were dried vigorously and placed and cared for in a closed infant incubator with humidified air: initially at 37 ° C and 70% humidity on day 1, 36 ° C and 60% humidity on day 2, and thereafter at 35 ° C and 50% humidity. At 2 h of age, the pups were weighed and hand-fed with 1 mL of kitten-milk replacement formula (KMR; PETAG Inc., USA) using a 3.5-Fr feeding tube, and every 12 h thereafter, the meals were increased by 0.5 mL. The term (T) pups were delivered at term by spontaneous vaginal delivery at gestational day 32, and then nursed and fed by their lactating doe. All pups were weighed once daily. The number of pups according to postnatal age in the PT and T groups is shown in Table 1. Mortality after inclusion in the study was 38% in the PT group and 0% in the T group.

Procedures for Blood and Tissue Sampling

Blood sampling was performed through cardiac puncture after sedation with isoflurane inhalation prior to in vivo perfusion fixation. Blood was collected in serum tubes and centrifuged at 1,000 *g* for 10 min at room temperature. The serum was then transferred into new tubes and stored at −80 ° C until analysis. Perfusion-fixation of the brain was performed by cardiac cannulation following thoracotomy and infusion of 0.9% saline followed by 4% paraformaldehyde (PFA). After complete perfusion, the cerebrum and cerebellum were carefully extracted from the skulls and immersed in 4% PFA. A change to fresh PFA was done after 3–6 h. Thereafter, the tissues were prepared for histochemical analysis as described below.

Serum IGF-1 Concentrations

The rabbit pup serum concentration of IGF-1 was determined using the human IGF-1 ELISA from Mediagnost (Reutlingen, Germany). The manufacturer has proved this assay

applicable for rabbit serum samples. The analysis was performed according to the manufacturer's instructions.

Tissue Preparation

The brains were fixated in 4% PFA for 48 h. Thereafter, they were dehydrated, cleared, and infiltrated with paraffin automatically in a TISSUE-TEK V.I.P. (Miles Scientific Corp., Newark, NJ, USA) and embedded in paraffin. The cerebellum was sectioned, and 4-μm sections in the parasagittal plane at the level of the dentate nucleus were made (Leica, RM2255 Microtome) and mounted on microscope slides and dried at 37 ° C for 12–16 h.

Immunohistochemical Staining

Following deparaffinization, the sections were antigen-retrieval pretreated by boiling in 0.05 M boric acid buffer (pH 8.0) for 20 min followed by 20 min acclimatization at room temperature. Sections were then incubated with the primary antibody; mouse anti Ki67 (diluted 1: 100, Dako, M7240), rabbit anti-cleaved caspase-3 (diluted 1: 100, Cell signaling, #9661), mouse anti-calbindin (diluted 1: 200, DBS, CB-855), rabbit anti-GFAP (diluted 1: 150, Abcam, ab16997), mouse anti-Olig-2 (diluted 1: 1,000, Millipore, MABN50), rabbit anti-Iba1 (diluted 1: 200, Biocare, CP290), or rabbit anti-sonic hedgehog (diluted 1: 200, Abcam, ab73958). All primary antibodies were diluted in PBS containing 5% normal goat serum (Jackson ImmunoResearch, 005-000-121) for 1 h at room temperature. Sections were then washed 3 times in PBS followed by incubation in corresponding secondary antibody, i.e. for rabbit primary antibodies: BrightVision rabbit/HRP (Immunologic, DPVR110HRP) and mouse primary antibodies: BrightVision mouse/HRP (Immunologic, DPVM110HRP), for 30 min. After being washed 3 times in Tris buffer (0.05 M, pH 7.6), the sections were incubated with DAB (diaminobenzidine, Sigma D5637-5G) for 5 min, counterstained with hematoxylin for 5 s, dehydrated and mounted in Pertex, and coverslipped. Mayer's hematoxylin and eosin (HE) staining was performed in a Leica ST4040 automatic stainer.

Microscope Analysis and Data Documentation

Microscope analysis was performed with a Leica light microscope (DMRX) equipped with a digital camera (MC120 HD, Leica).

Histological Analysis

Analysis of the EGL was performed in 4 predefined regions: the inner and outer portion of lobule V, and the inner and outer portion of lobule IX, respectively (Fig. 1). These regions were chosen as the regions with possible maturational differences in EGL proliferation and in subsequent width. Measurement of the width of the proliferative EGL, as constituted by Ki67-positive cells, was performed by using the ×40 objective lens on the Leica DMRX microscope. The average of the 4 respective measured widths was calculated for each pup. Ki67-negative cells were regarded as differentiated, and were counted over an area of 100 μm. Qualitative evaluation was performed of Purkinje cell (calbindin immunoreactivity) and Bergmann glia morphology (GFAP immunoreactivity) at repeated postnatal ages in both the PT and T groups. Distribution and the presence of immunoreactivity for cleaved caspase-3 and Shh were described qualitatively.

Using the Leica Q500 image analysis system of the microscope, the area of calbindin-positive-stained cells was determined in relation to the area of the molecular layer. Thus, calbindin staining was expressed as percentage positive area in relation to a standardized area of the molecular layer. Nonspecific background staining was taken into consideration.

Cerebellar White-Matter Damage

Cerebellar white-matter impairment was evaluated in PT and T pups by HE staining. We further performed qualitative and quantitative analysis of immunostaining for Ki67, Olig2, and Iba1, for determination of cell proliferation and presence of oligodendroglial and microglial cells in PT and T pups.

Antibody Control for Immunohistochemical Staining

Antibody specificity tests were performed on parallel sections in all labeling experiments in which the primary antibodies were excluded from the labeling protocol (online suppl. Fig. 1; see www.karger.com/doi/10.1159/000480428 for all online suppl. material). This confirmed that the visualized and documented immunohistochemical staining was caused by the binding of the respective primary antibodies, not to the binding of secondary antibodies.

Statistics

Statistics were performed with IBM SPSS v21 for Microsoft Windows (IBM, Armonk, NY, USA). Differences between groups and time points were analyzed with the Mann-Whitney U test. Correlations between continuous variables were analyzed with regression analysis and adjustment for other variables was performed with multivariate regression analysis. $p < 0.05$ was considered significant.

Results

Weight Development

Preterm birth was associated with profound growth restriction (Fig. 2A). The mean weight of the PT group was less than that of the T group at each time point (all $p < 0.05$). The mean (±SD) weight of the PT group exhibited no increase in weight from birth at E29 to P0, i.e. 40 (±3) versus 39 (±2) g. Mean relative increase in weight from P0 to P9 was 3 times higher in the T group ($p < 0.01$; 246% in the T group vs. 83% in the PT group). No catch-up in weight in the PT group was noted during the observation period.

Serum IGF-1

Mean protein levels of circulating IGF-1 were lower in the PT group than in the T group at P0, P2, and P9 (all $p < 0.05$; Fig. 2B). Mean serum values generally increased with increasing postnatal age in PT and in T pups, although a decrease was observed in mean serum IGF-1 level in the PT group at P9 compared to at P5 ($p < 0.05$). Concentrations of serum IGF-1 were highly correlated with weight ($r^2 = 0.89$, $p < 0.001$). This association remained significant ($p < 0.001$) after adjustment for gestational age at birth and for postnatal age.

Cerebellar Histology

EGL Measurements—There was no significant difference in the total width of the EGL between the PT and T groups. The total EGL width was largest at P0 in both groups and decreased at subsequent time points (Fig. 3A). The mean (±SD) Ki67-positive portion of the EGL was reduced at P2 in the PT group, i.e. 35 (±3) μm, versus in the T group, 44 (±4) μm ($p = 0.01$; Fig. 3B). The mean Ki67-positive layer had its maximal width at P0 in the PT group and was decreased at P2 ($p < 0.05$). The corresponding decrease from maximal Ki67-positive width appeared later in the T group, between P2 and P5. The number of Ki67-negative cells in the EGL did not differ between the PT and T group at any of the observed time points (Fig. 3C).

Purkinje Cell Maturation and Sonic Hedgehog Expression—Purkinje cell appearance, as determined by calbindin staining, changed strikingly over time, with an organized monolayer of cell somata visible at P5, and still more defined at P9, in PT and T pups. Dendritic length and arborization increased with increasing postnatal age. Calbindin staining was less intense and Purkinje cell morphology was clearly affected in the PT group at P0 and P2, with reduced arborization and dendritic spines compared to in the T group (Fig. 4). Quantitative analysis showed a clear decrease in percentage calbindin-labeled Purkinje cell area in the PT pups compared to in the T pups at P0 ($p = 0.003$), P2 ($p = 0.004$), and P5 ($p = 0.04$).

Staining for Shh revealed no clear difference between the PT and T groups. At earlier time points, it was more scattered and less pronounced in Purkinje cells and also visible within the EGL and the IGL. With increasing postnatal age, it was more intense and mainly confined to the cytoplasm of the Purkinje cell somata (at P5 and P9; Fig. 4).

Bergmann Glia—At E29, GFAP-positive glial fibers were poorly defined and very scarce. From P0 onwards, no obvious differences could be observed between the PT and T groups. With increasing postnatal age, the glial fibers were increasingly confined to the molecular layer (Fig. 5).

Cleaved Caspase-3—Staining for cleaved caspase-3 was positive in Bergmann glial fibers at E29, P0, and P2, and most pronounced at the interface between the inner EGL and the molecular layer. At later time points, i.e. P5 and P9, staining for cleaved caspase-3 was restricted to the somata of cells, with localization suggestive of Bergmann glia (Fig. 5).

Staining for cleaved caspase-3 was not observed in the EGL or in other cellular populations, apart from those with a Bergmann glia appearance. No difference in cleaved caspase-3 staining was observed between the PT and T pups.

Cerebellar White-Matter Impairment—At P2 and P5, several of the PT pups exhibited signs of damage localized to the cerebellar white matter, which was not observed in the T group (Fig. 6). Quantitative densitometric analysis in PT and T pups at P2 showed a reduction in Olig 2-positive cells in cerebellar white matter ($p = 0.009$) and a decrease in proliferating Ki67-positive cells ($p = 0.03$). Immunostaining with Iba1 revealed an increased

number of Iba1-positive microglia ($p = 0.04$) in cerebellar white matter, with an activated ameboid morphology compared to ramified, quiescent cells in the T pups (Fig. 6).

Discussion

We have shown that preterm birth in the rabbit pup mimics birth in the very preterm human infant in several relevant aspects. Cesarean section of the pregnant doe, 3 days prior to vaginal delivery, was associated with postnatal growth restriction and with decreased postnatal circulating levels of IGF-1 in preterm rabbit pups. These findings were accompanied by changes in EGL proliferation and cerebellar Purkinje cell morphology, indicating affected or impaired cerebellar development. Of note, we also observed signs of cerebellar white-matter damage in a subgroup of preterm rabbit pups.

The vast majority of studies aiming to evaluate the consequences of insults in the very immature brain have used mice or rat models. These rodents, when studied at postnatal age P2–P7, exhibit a varying degree of brain immaturity reflecting that of the human preterm brain from extreme prematurity to a maturity corresponding to term age [16]. However, there is strong support that the harmful influence of very preterm birth on brain development is related to systemic alterations due to premature loss of the maternal/fetal interaction, e.g., placental support and trophic deprivation due to less than optimal postnatal nutrition [17]. An animal model that incorporates both brain immaturity per se and trophic deprivation due to loss of placental support would thus seem essential in order to generate knowledge which can be translated to the preterm human infant. The preterm rabbit pup model has primarily been used by us and other study groups for the study of cerebral intraventricular hemorrhage [10, 18]. Unlike other rodent models, it incorporates premature loss of placental support, so we aimed to evaluate aspects of trophic deprivation, i.e. circulating levels of IGF-1 and postnatal weight development.

Preterm birth in rabbit pups was followed by decreased circulating levels of IGF-1 and by postnatal growth restriction. Circulating levels of IGF-1 were highly correlated to body weight independently of postnatal age and maturity at birth. These results correspond well to what we and other authors have shown in preterm human infants [17]. Very preterm infants have low levels of IGF-1 after birth and generally exhibit an increase at around 30 weeks' gestation which coincides with the initiation of catch-up growth. Variations in protein and caloric intake have a limited influence on circulating IGF-1 during the initial phase of growth restriction but a significant influence on the IGF-1 levels during established catch-up growth. The rabbit pups in this study received a nutritional intake relative to weight very similar to that administered to human infants. The group of term pups that served as a reference group for normal growth received milk from their lactating doe. The study was not designed to evaluate the impact of varied nutrition on either IGF-1 or on body growth. Although body weight increased with increasing postnatal age in PT pups, there was no sign of accelerated catch-up growth. The observed decrease in serum IGF-1 from P5 to P9 was most likely representative of a relative nutritional deficit.

IGF-1, by acting through the IGF-1 receptor, influences all of the mechanisms in normal brain development apart from migration, i.e. proliferation, differentiation, maturation, and

apoptosis [19–21]. The growth factor IGF-1 is predominantly expressed in neurons and is enrolled in progenitor proliferation and neuronal outgrowth in the cerebellum [22]. IGF-1 has been shown to act on the survival of the Purkinje cells via an antiapoptotic effect [22] and also on the proliferation of the granule cell precursors [23]. The decrease in circulating levels of IGF-1 following the loss of placental support at preterm birth in human infants is associated with lower brain volumes at term age with a positive correlation to cerebellar volume [4].

The cerebellum is the fastest-growing part of the brain during the last trimester of human gestation and is in a very active proliferation phase before reaching term age which suggest a heightened vulnerability to environmental changes [8, 12]. Indeed, we have shown that cerebellar growth at term age, as detected by volumetric magnetic resonance imaging, exhibits a stronger association with postnatal growth and longitudinal levels of circulating IGF-1 than that of the supratentorial brain in very preterm infants [4]. Effects of trophic deprivation in the immature cerebellum have primarily been studied in animal models of intrauterine growth restriction (IUGR). IUGR induced by uterine artery ligation in the guinea-pig leads to a significant reduction in the number of Purkinje cells and the volume of the molecular layer, the internal granular layer, and the cerebellar white matter [24].

In humans, placental insufficiency has been shown to alter brain development following IUGR [25] and to reduce the number of Purkinje cells in the cerebellum [24].

The longitudinal evaluation of total and proliferative EGL width in rabbit pups showed that total EGL width was maximal at P0 in both groups and decreased thereafter. Measure of the proliferative portion of the EGL, as determined by Ki67-positive staining, indicated that proliferation was maximal around P0–P2. The finding that the PT group exhibited a decreased proliferative layer at P2 was not unexpected, as the period of maximal proliferation during development probably represents a time point of heightened vulnerability. Our observations of the EGL of rabbit pups are similar to those described in human cerebellar maturation; the EGL was thickest at P0, which is analogous to the developmental stage of the human fetal brain at 25 weeks' gestation when it reaches its peak thickness and is highly proliferative [12].

We observed altered Purkinje cell morphology clearly in the PT group, with decreased calbindin staining, reduced cell somata size, and decreased arborization. These morphological changes were most prominent at P0 and P2, coinciding in time with the finding of decreased EGL proliferation. The vulnerability of Purkinje cell development to insults associated with preterm birth have been recently shown in rat pups exposed to neonatal hyperoxia and also in preterm rabbit pups with preterm cerebral intraventricular hemorrhage exhibiting delayed maturation of Purkinje cells and decreased granular precursor cell proliferation [26, 27]. The cerebellar Purkinje cells have several key functions relating to EGL proliferation, and subsequent inward cell migration and Purkinje cell secretion of the transcription factor Shh are key for EGL precursor cell proliferation [12, 13, 28]. We did not detect any clear differences in Shh staining between the PT and T groups, and thus do not have evidence of Purkinje cell degeneration leading to impaired or reduced Shh-induced proliferation. However, our evaluation was restricted to the ligand Shh whereas

alterations in other key players, such as the Patched receptor on granule precursor cells or intracellular mediators of transcription, may be involved in decreased granule cell proliferation.

We observed that Shh was diffusely present in the EGL and inner layers at earlier time points, and that with increasing postnatal age it became increasingly confined to an organized monolayer of Purkinje cell somata. This maturational pattern has previously been observed in mice and in human embryos [16, 28].

We hypothesized that events relating to premature exposure to the postnatal environment would induce mechanisms leading to apoptosis in the rapidly proliferating cerebellum. This was not observed, as determined by staining for cleaved caspase-3. However, we did detect positive staining for cleaved caspase-3 which was restricted to the Bergmann glia. Previous studies have demonstrated that active caspase-3 has a role of inducing and maintaining differentiation of the Bergmann glia during normal cerebellar development [29–31]. The distribution and staining pattern over time in Bergmann glia did not differ between PT and T pups.

Finally, we observed clear signs of damage in the cerebellar white matter in PT pups. This damage was characterized by a reduction in Olig2-staining oligodendrocytes, a reduced number of proliferating Ki67-positive cells, and an increased presence of Iba1-positive microglia with an activated morphology. These findings are very similar to those observed in immature, periventricular, supratentorial white matter following exposure to proinflammatory or hyperoxic insults [32, 33]. Less is known about the possible intrinsic vulnerability of the cerebellar white-matter preoligodendrocyte population. Of note, selective cerebellar white-matter volume reduction has been observed in adolescents with a history of very preterm birth and prenatal growth restriction (pers. communication).

In conclusion, we show that the preterm rabbit pup model exhibits a combination of characteristics relevant to human preterm birth. Our study is descriptive and causality can thus not be inferred between our observations of decreased growth, circulating IGF-1, and alterations in key cerebellar cell populations suggestive of impaired cerebellar development. Future studies on this animal model will focus on relating our observations to long-term functional evaluation. We also propose the preterm rabbit pup model as appropriate for the study of relationships between nutritional modification, pharmacological intervention, and short- and long-term neurodevelopment.

Supplementary Material

Refer to Web version on PubMed Central for supplementary material.

Acknowledgments

This work was supported by the Swedish Research Council, governmental ALF research grants to Lund University and Lund University Hospital, the European Commission (FP7, Project 305485 PREVENT-ROP), the Crafoordska Foundation, the Greta and Johan Kock Foundation, the Alfred Österlund Foundation, the Erasmus Mundus Fetalmed-PhD Program, and the Fanny Ekdahls Foundation. The authors wish to acknowledge Carin Sjölund from Lund University, for excellent technical assistance.

References

1. Wood NS, Marlow N, Costeloe K, Gibson AT, Wilkinson AR. EPICure Study Group: Neurologic and developmental disability after extremely preterm birth. N Engl J Med. 2000; 343:378–384. [PubMed: 10933736]
2. Marret S, Marchand-Martin L, Picaud JC, Hascoët JM, Arnaud C, Rozé JC, Truffert P, Larroque B, Kaminski M, Ancel PY. EPIP-AGE Study Group: Brain injury in very preterm children and neurosensory and cognitive disabilities during childhood: the EPIPAGE cohort study. PLoS One. 2013; 8:e62683. [PubMed: 23658763]
3. Serenius F, Källen K, Blennow M, Ewald U, Fellman V, Holmstrom G, Lindberg E, Lundqvist P, Maršál K, Norman M, Olhager E, Stigson L, Stjernqvist K, Vollmer B, Strömberg B. EXPRESS Group: Neurodevelopmental outcome in extremely preterm infants at 2.5 years after active perinatal care in Sweden. JAMA. 2013; 309:1810–1820. [PubMed: 23632725]
4. Hansen-Pupp I, Hövel H, Hellström A, Hellström-Westas L, Löfqvist C, Larsson EM, Lazeyras F, Fellman V, Hüppi PS, Ley D. Post-natal decrease in circulating insulin-like growth factor-I and low brain volumes in very preterm infants. J Clin Endocrinol Metab. 2011; 96:1129–1135. [PubMed: 21289247]
5. Messerschmidt A, Brugger PC, Boltshauser E, Zoder G, Sterniste W, Birnbacher R, Prayer D. Disruption of cerebellar development: potential complication of extreme prematurity. Am J Neuroradiol. 2005; 26:1659–1667. [PubMed: 16091510]
6. Tam EW, Ferriero DM, Xu D, Berman JI, Vigneron DB, Barkovich AJ, Miller SP. Cerebellar development in the preterm neonate: effect of supratentorial brain injury. Pediatr Res. 2009; 66:102–106. [PubMed: 19287350]
7. Tam EW, Rosenbluth G, Rogers EE, Ferriero DM, Glidden D, Goldstein RB, Glass HC, Piecuch RE, Barkovich AJ. Cerebellar hemorrhage on magnetic resonance imaging in preterm newborns associated with abnormal neurologic outcome. J Pediatr. 2011; 158:245–250. [PubMed: 20833401]
8. Limperopoulos C, Soul JS, Gauvreau K, Huppi PS, Warfield SK, Bassan H, Robertson RL, Volpe JJ, du Plessis AJ. Late gestation cerebellar growth is rapid and impeded by premature birth. Pediatrics. 2005; 115:688–695. [PubMed: 15741373]
9. Vinukonda G, Csiszar A, Hu F, Dummula K, Pandey NK, Zia MT, Ferreri NR, Ungvari Z, LaGamma EF, Ballabh P. Neuroprotection in a rabbit model of intraventricular haemorrhage by cyclooxygenase-2, prostanoid receptor-1 or tumour necrosis factor-alpha inhibition. Brain. 2010; 133:2264–2280. [PubMed: 20488889]
10. Chua CO, Chahboune H, Braun A, Dummula K, Chua CE, Yu J, Ungvari Z, Sherbany AA, Hyder F, Ballabh P. Consequences of Intraventricular hemorrhage in a rabbit pup model. Stroke. 2009; 40:3369–3377. [PubMed: 19661479]
11. Hansen-Pupp I, Hövel H, Lofqvist C, Hellström-Westas L, Cilio CM, Andersson S, Fellman V, Ley D. Circulatory insulin-like growth factor-I and brain volumes in relation to neurodevelopmental outcome in very preterm infants. Pediatr Res. 2013; 74:564–569. [PubMed: 23942554]
12. Volpe JJ. Cerebellum of the premature infant: rapidly developing, vulnerable, clinically important. J Child Neurol. 2009; 24:1085–1104. [PubMed: 19745085]
13. Dahmane N, Ruiz i Altaba A. Sonic hedgehog regulates the growth and patterning of the cerebellum. Development. 1999; 126:3089–3100. [PubMed: 10375501]
14. Langford K, Nicolaides K, Miell JP. Maternal and fetal insulin-like growth factors and their binding proteins in the second and third trimesters of human pregnancy. Hum Reprod. 1998; 13:1389–1393. [PubMed: 9647578]
15. Fernandez C, Tatard VM, Bertrand N, Dahmane N. Differential modulation of sonic hedgehog-induced cerebellar granule cell precursor proliferation by the IGF signaling network. Dev Neurosci. 2010; 32:59–70. [PubMed: 20389077]
16. Haldipur P, Bharti U, Govindan S, Sarkar C, Iyengar S, Gressens P, Mani S. Expression of sonic hedgehog during cell proliferation in the human cerebellum. Stem Cells Dev. 2012; 21:1059–1068. [PubMed: 21732818]

17. Hansen-Pupp I, Löfqvist C, Polberger S, Niklasson A, Fellman V, Hellström A, Ley D. Influence of insulin-like growth factor I and nutrition during phases of postnatal growth in very preterm infants. Pediatric Research. 2011; 69:448–453. [PubMed: 21263374]

18. Sveinsdóttir S, Cinthio M, Ley D. High-frequency ultrasound in the evaluation of cerebral intraventricular haemorrhage in preterm rabbit pups. Ultrasound Med Biol. 2012; 38:423–431. [PubMed: 22305058]

19. Carson MJ, Behringer RR, Brinster RL, Mc-Morris FA. Insulin-like growth factor I increases brain growth and central nervous system myelination in transgenic mice. Neuron. 1993; 10:729–740. [PubMed: 8386530]

20. Chrysis D, Calikoglu AS, Ye P, D'Ercole AJ. Insulin-like growth factor-I overexpression attenuates cerebellar apoptosis by altering the expression of Bcl family proteins in a developmentally specific manner. J Neurosci. 2001; 21:1481–1489. [PubMed: 11222638]

21. O'Kusky JR, Ye P, D'Ercole AJ. Insulin-like growth factor-I promotes neurogenesis and synaptogenesis in the hippocampal dentate gyrus during postnatal development. J Neurosci. 2000; 20:8435–8442. [PubMed: 11069951]

22. Croci L, Barili V, Chia D, Massimino L, van Vugt R, Masserdotti G, Longhi R, Rotwein P, Consalez GG. Local insulin-like growth factor I expression is essential for Purkinje neuron survival at birth. Cell Death Differ. 2011; 18:48–59. [PubMed: 20596079]

23. Ye P, Xing Y, Dai Z, D'Ercole AJ. In vivo actions of insulin-like growth factor-I (IGF-I) on cerebellum development in transgenic mice: evidence that IGF-I increases proliferation of granule cell progenitors. Brain Res Dev Brain Res. 1996; 95:44–54. [PubMed: 8873975]

24. Mallard C, Loeliger M, Copolov D, Rees S. Reduced number of neurons in the hippocampus and the cerebellum in the postnatal guinea-pig following intrauterine growth-restriction. Neuroscience. 2000; 100:327–333. [PubMed: 11008170]

25. Tolsa CB, Zimine S, Warfield SK, Freschi M, Sancho Rossignol A, Lazeyras F, Hanquinet S, Pfizenmaier M, Huppi PS. Early alteration of structural and functional brain development in premature infants born with intrauterine growth restriction. Pediatr Res. 2004; 56:132–138. [PubMed: 15128927]

26. Scheuer T, Sharkovska Y, Tarabykin V, Marggraf K, Brockmoller V, Buhrer C, Endesfelder S, Schmitz T. Neonatal hyperoxia perturbs neuronal development in the cerebellum. Mol Neurobiol. 2017 E-pub ahead of print.

27. Agyemang AA, Sveinsdóttir K, Vallius S, Sveinsdóttir S, Bruschettini M, Romantsik O, Hellström A, Smith LEH, Ohlsson L, Holmqvist B, Gram M, Ley D. Cerebellar exposure to cell-free hemoglobin following preterm intraventricular hemorrhage: causal in cerebellar damage? Transl Stroke Res. 2017 Epub ahead of print.

28. Lewis PM, Gritli-Linde A, Smeyne R, Kottmann A, McMahon AP. Sonic hedgehog signaling is required for expansion of granule neuron precursors and patterning of the mouse cerebellum. Dev Biol. 2004; 270:393–410. [PubMed: 15183722]

29. Oomman S, Strahlendorf H, Finckbone V, Strahlendorf J. Non-lethal active caspase-3 expression in Bergmann glia of postnatal rat cerebellum. Brain Res Dev Brain Res. 2005; 160:130–145. [PubMed: 16226814]

30. Oomman S, Strahlendorf H, Dertien J, Strahlendorf J. Bergmann glia utilize active caspase-3 for differentiation. Brain Res. 2006; 1078:19–34. [PubMed: 16700096]

31. Finckbone V, Oomman SK, Strahlendorf HK, Strahlendorf JC. Regional differences in the temporal expression of non-apoptotic caspase-3-positive Bergmann glial cells in the developing rat cerebellum. Front Neuroanat. 2009; 3:1–7. [PubMed: 19169410]

32. Gerstner B, DeSilva TM, Genz K, Armstrong A, Brehmer F, Neve RL, Felderhoff-Mueser U, Volpe JJ, Rosenberg PA. Hyperoxia causes maturation-dependent cell death in the developing white matter. J Neurosci. 2008; 28:1236–1245. [PubMed: 18234901]

33. Supramaniam V, Vontell R, Srinivasan L, Wyatt-Ashmead J, Hagberg H, Rutherford M. Microglia activation in the extremely preterm human brain. Pediatr Res. 2013; 73:301–309. [PubMed: 23364172]

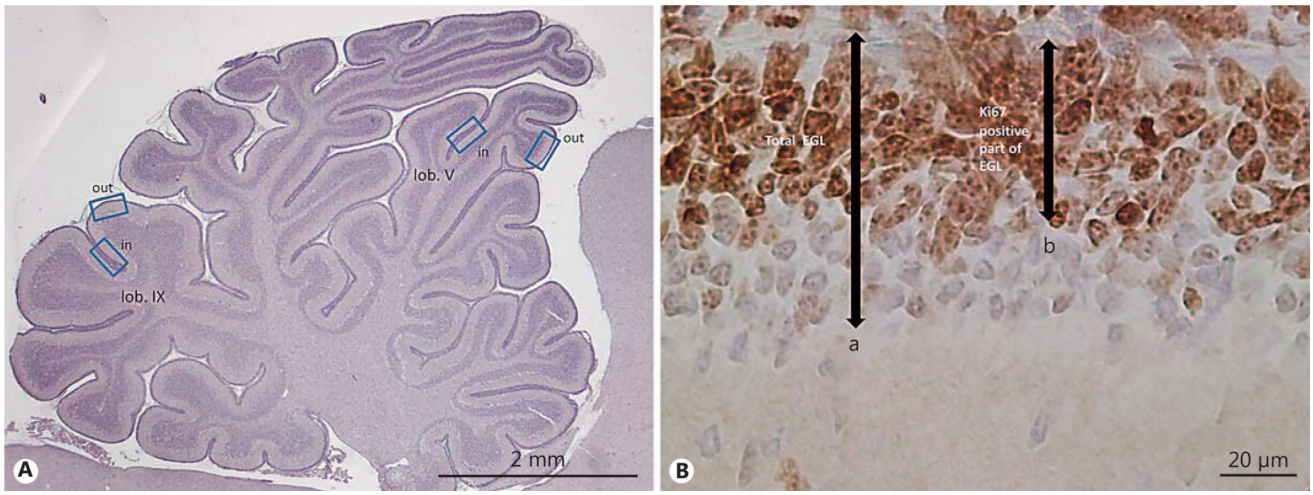

Fig. 1.

Measurement of external granular layer (EGL) width. **A** Cerebellar overview illustrating areas (outward and inward regions of lobuli V and IX) used for quantitative measurement of total and proliferative EGL width. **B** HE- and Ki67-stained section of the EGL illustrating measurements obtained for quantitative EGL analysis: (a) total EGL = width of proliferative EGL + inner zone of differentiated granular precursor cell (GPC) layer, and (b) proliferative EGL = width of Ki67-positive proliferating GPC layer.

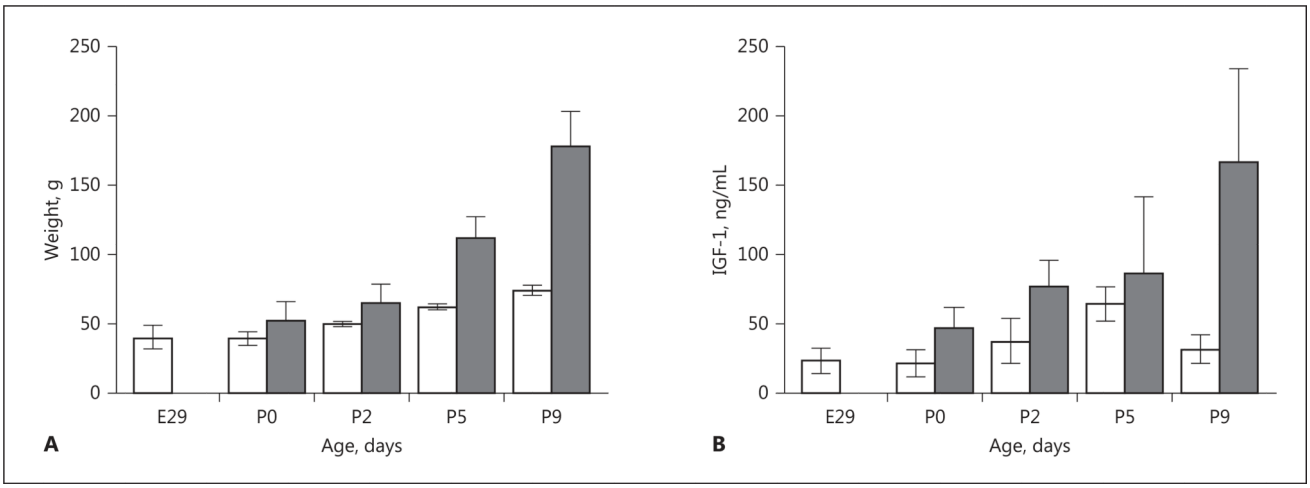

Fig. 2.

Growth and serum insulin-like growth factor 1 (IGF-1) in preterm (PT) and term (T) rabbit pups. **A** Rabbit pups were weighed daily. The mean weight in the PT group (white bars) was lower than in the T group (grey bars) at all postnatal time points ($p < 0.05$). Error bars denote 1 SD. **B** Blood for analysis was retrieved at termination of PT and T pups at each respective postnatal time point, and analyzed according to the description in Material and Methods. Mean levels of serum IGF-1 were lower in the PT group (white bars) than in the T group (grey bars) at all time points (all $p < 0.05$). Error bars denote 1 SD. Differences in weight and serum IGF-1 between groups were analyzed using the Mann-Whitney U test.

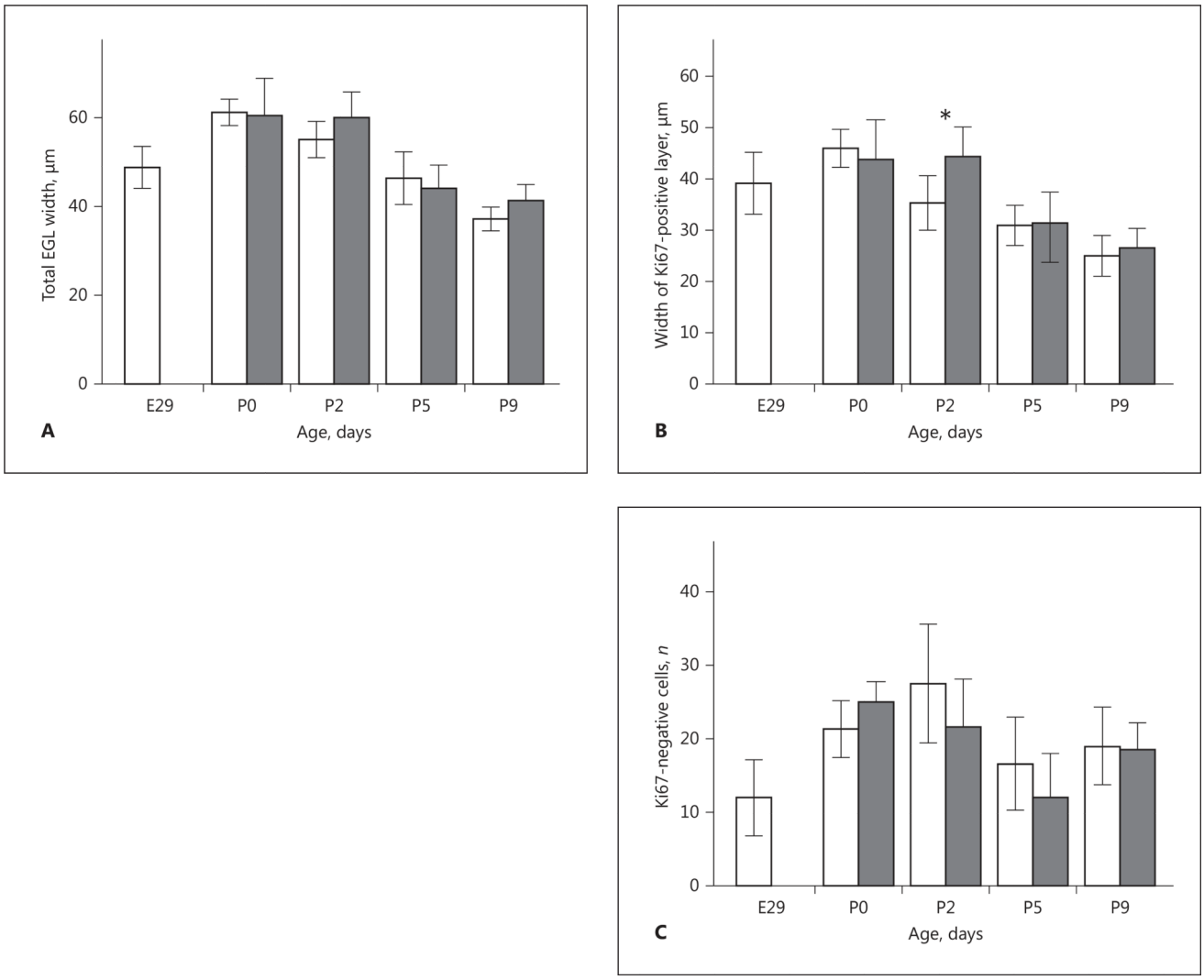

Fig. 3.

Cerebellar external granular layer (EGL) width in preterm (PT; white bars) and term (T; grey bars) rabbit pups. Measurement of total and proliferative EGL width was performed using bright-field microscopy in defined regions of cerebellar lobuli V and IX during postnatal development as described in Material and Methods. **A** The total width of the EGL did not differ between the PT and T groups at any postnatal time point. Total EGL was thickest at P0 in both groups and exhibited a continuous decrease at subsequent time points. Error bars denote 1 SD. **B** At P2, the mean (±SD) width of the proliferative layer of the EGL was decreased in the PT group 35 (±3) µm compared to the T group 44 (±4) µm. $p = 0.01$. Error bars denote 1 SD. **C** The number of differentiated (Ki67-negative) cells did not differ between the PT and T rabbit pups at any postnatal time point.

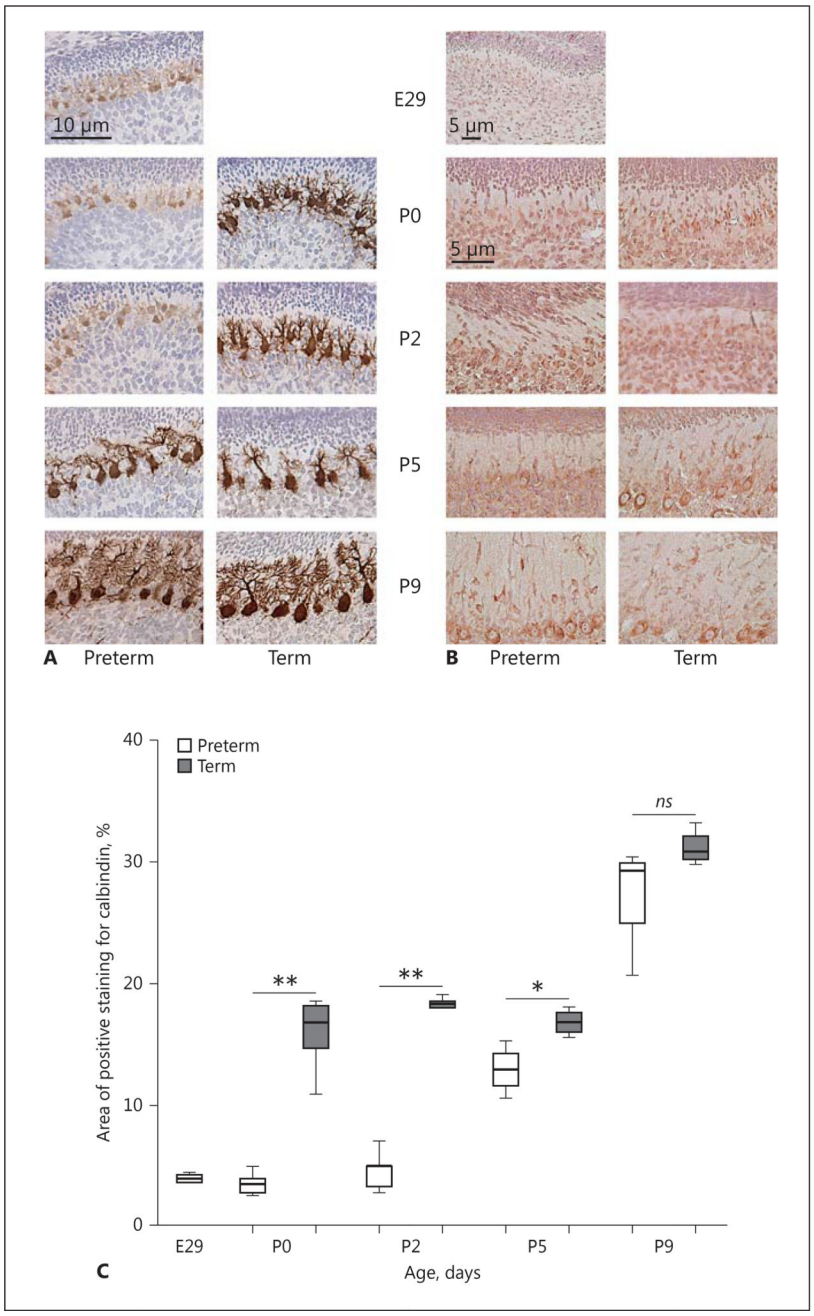

Fig. 4.

Cerebellar Purkinje cell development and Sonic hedgehog (Shh) expression in preterm (PT) and term (T) rabbit pups. **A** The development of Purkinje cells was evaluated by their morphology as determined by calbindin staining using a bright-field microscope as described in Material and Methods. Cell maturity over time, i.e. dendritic length and arborization, and their formation into the Purkinje cell layer were compared between the 2 groups at each postnatal time point. Representative immunosections of Purkinje cell morphology in PT and T pups are shown at each postnatal time point and also the progressive maturation from a fuciform to a stellate state. Calbindin staining (brown) was

decreased in the PT group at P0 and P2 (vs. in the T group), with reduced arborization and dendritic spines. **B** Immunostaining for Shh was performed in sections from PT and T pups at each postnatal time point as described in Material and Methods. The pattern and intensity of staining for Shh were similar in the PT and T groups. Shh staining was scattered and present within the external granular layer, like in the internal granular layer, at early postnatal time points, and was restricted to the Purkinje cell somata (brown) at later time points. Scale bar, 50 μm. **C** Quantitative analysis of calbindin staining showed a decrease in the area (%) of calbindin-labeled Purkinje cells in the PT pups versus in the T pups at P0 ($p = 0.003$), P2 ($p = 0.004$), and P5 ($p = 0.04$).

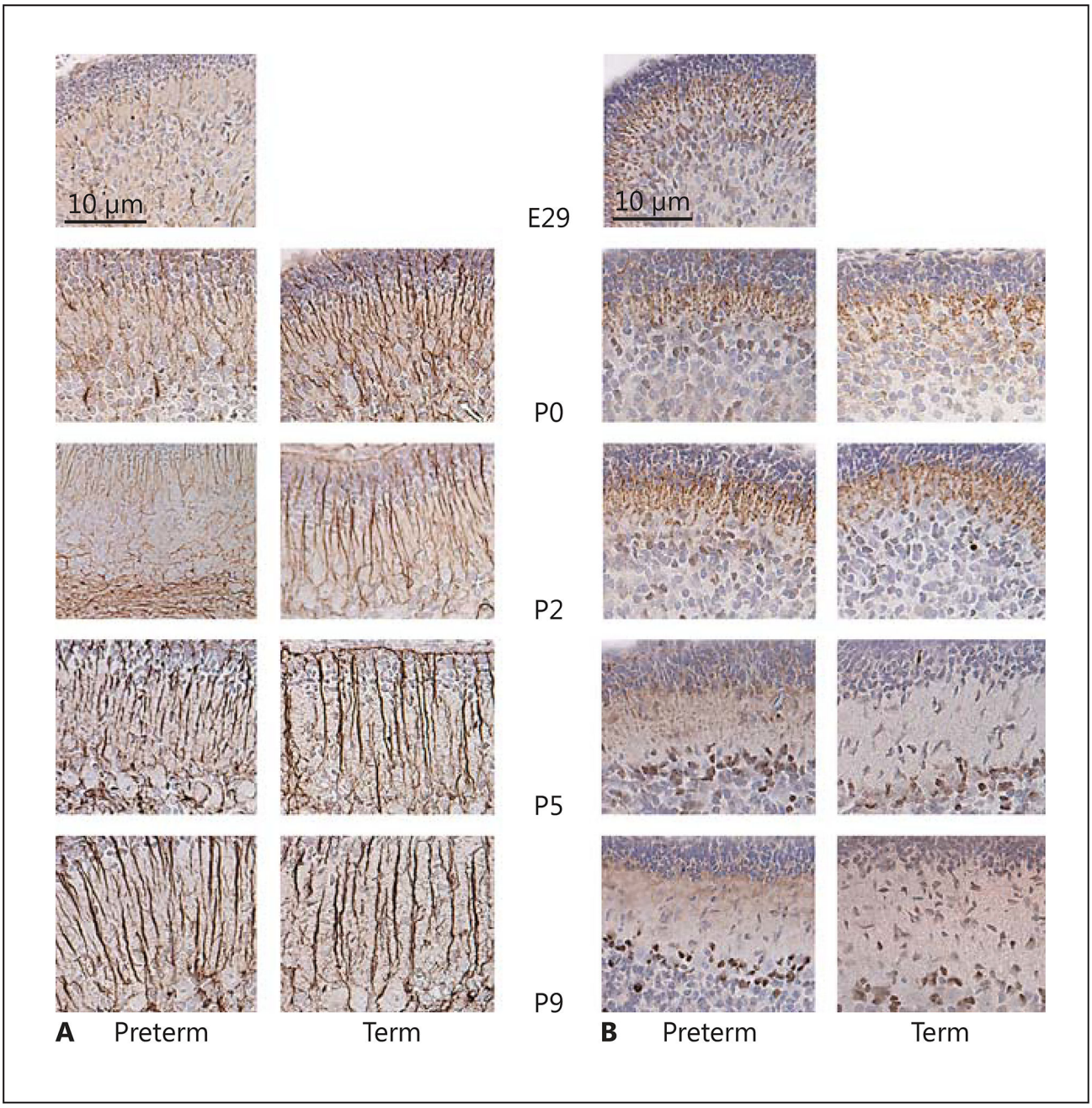

Fig. 5.

Cerebellar Bergman glia development and expression of cleaved caspase-3 in preterm (PT) and term (T) rabbit pups. **A** Immunostaining with GFAP was used to evaluate Bergman glia development in PT and T rabbit pups at each postnatal time point as described in Material and Methods. No clear differences in Bergman glia morphology were observed between the PT and T groups. At E29, GFAP-positive glial fibers were poorly defined and very scarce. With increasing postnatal age, glial fibers become more developed and confined to the molecular layer. **B** Staining for cleaved caspase-3 was applied to evaluate possible apoptosis during cerebellar development in the PT and T groups, as described in Material and

Methods. Positive staining for cleaved caspase-3 (brown) was restricted to the radial fibers of the Bergman glia at E29, P0, and P2, and was predominantly located at the interface between the inner external granular layer and the molecular layer. At P5 and P9, staining for cleaved caspase-3 was restricted to the somata of cells, with a localization suggestive of Bergmann glia. The staining pattern for cleaved caspase-3 suggested a constitutive expression during Bergmann glia development and did not differ between the PT and T groups. Scale bar, 10 μm.

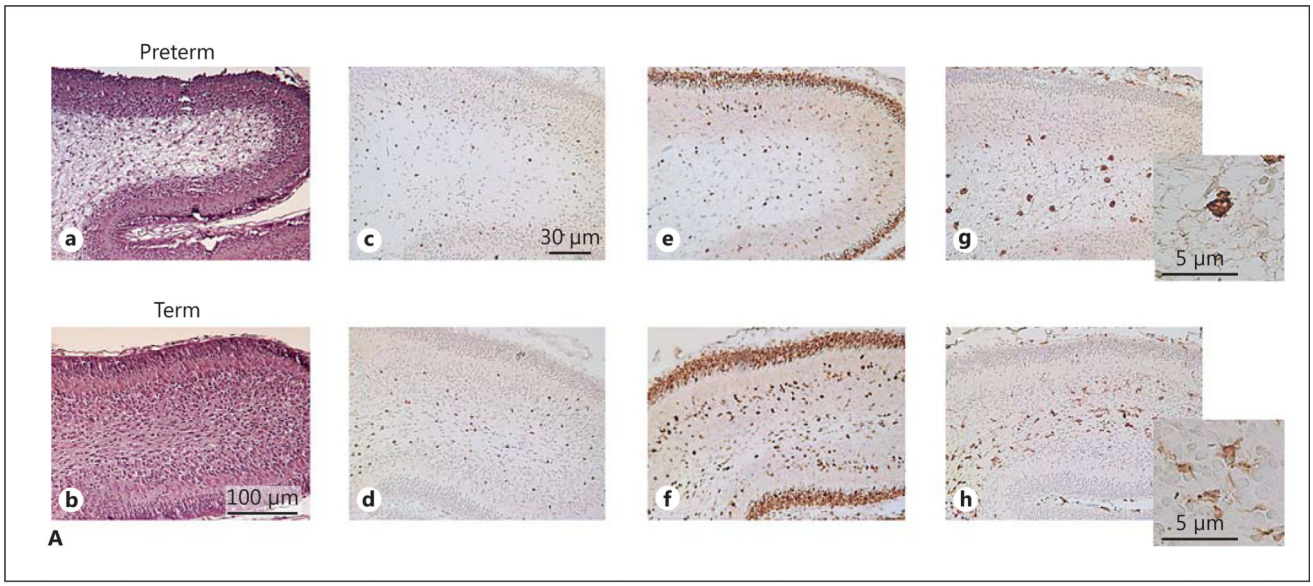

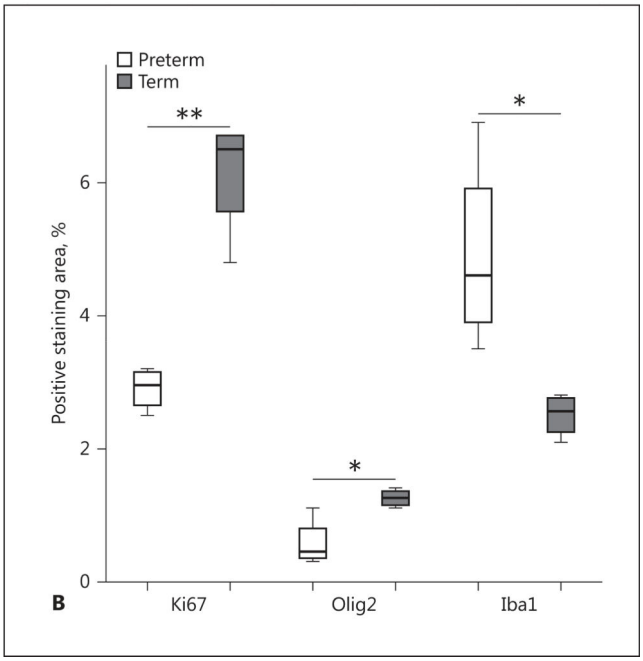

Fig. 6.

Cerebellar white-matter damage in preterm (PT) rabbit pups. **A** Cerebellar sections exhibited signs of cellular damage in cerebellar white matter in PT pups at P2 and P5. HE. Cerebellar white-matter damage was not observed in T pups. Immunostaining with antibodies against Olig2, Ki-67, and Iba1, respectively, were performed as described in Material and Methods to characterize proliferation and oligodendroglial and microglial cellular response in cerebellar white matter in PT and T rabbit pups. Upper row: HE (**a**), Olig2 (**c**), Ki67 (**e**) and Iba1 (**g**) staining, respectively, in a representative PT rabbit pup at P2. Signs of white-matter damage in the HE-stained section correspond to a marked reduction of proliferating cells, a reduced number of Olig2-positive cells, and an increased number of Iba1-positive microglia

in the cerebellar white matter. Lower row: the corresponding immunostainings in a T pup at P2 (**b, d, f, h**) with no signs of white-matter damage for comparison. Scale bars: 100 μm (HE); 30 μm (Ki67, Olig2, and Iba1). **Insets** An activated ameboid Iba1-positive microglial morphology in the PT pup (**g**) compared to a quiescent ramified morphology in the T pup (**h**). **B** Quantitative analysis showed a decrease in staining for Olig2 (** $p = 0.009$) and Ki67 (* $p = 0.03$) and an increase in staining for Iba1 (* $p = 0.04$).

Table 1

Number of rabbit pups according to experimental group and postnatal age

	E29	P0	P2	P5	P9
Preterm pups	8	8	5	6	5
Term pups		10	10	6	6

E29, day of birth for preterm pups delivered by cesarean section; P0, day of birth for vaginally delivered term control pups and term equivalent age for preterm pups; P, postnatal day.